Received: 7 October 2022 | Accepted: 30 December 2022

DOI: 10.1002/pamm.202200149

Investigations on Guided Ultrasonic Wave Dispersion Behavior in Fiber Metal Laminates Using Finite Element Eigenvalue Analysis

Tilmann Barth[1,*], **Johannes Wiedemann**[2], **Thomas Roloff**[2], **Christian Hühne**[2,3], **Michael Sinapius**[2], and **Natalie Rauter**[1]

[1] Helmut-Schmidt-University / University of the Federal Armed Forces Hamburg, Institute of Mechanics, Holstenhofweg 85, 22043 Hamburg, Germany

[2] TU Braunschweig, Institute of Mechanics and Adaptronics, Langer Kamp 6, 38106 Braunschweig, Germany

[3] DLR, Institute of Composite Structures and Adaptive Systems, Lilienthalplatz 7, 38108 Braunschweig, Germany

Composite materials such as fiber metal laminates combine the advantages of metallic materials and fiber-reinforced polymers. Hence, these materials are of great interest for thin-walled structures in lightweight engineering. Due to the structure of these materials, damage to fiber metal laminate components occur more frequently inside the structure than with conventional materials. Since the detection of interlaminar damage is more complicated compared to external damage, it is one of the biggest challenges in the use of fiber metal laminates. One approach to detect this kinds of damage, is the use of guided ultrasonic waves, for example Lamb waves. To be able to perform such damage detection, knowledge about the propagation behavior of this kind of waves in fiber metal laminates is fundamental. Abrupt stiffness variations across the thickness of fiber metal laminates, resulting from the different material layers, lead to the question whether the known approaches for the propagation of guided ultrasonic waves in isotropic and transversely isotropic materials are applicable here. Therefore, the objective of this work is to investigate the propagation behavior of these guided ultrasonic waves in fiber-metal laminates over large frequency ranges. For this purpose, dispersion relations from finite element simulations are compared with experimental data and numerical solutions based on the analytical framework. The investigations are carried out using a fiber metal laminate consisting of steel and carbon fiber-reinforced polymers. Due to the orthotropy of the laminate, wave propagation in the fiber direction and perpendicular to it is considered. For the finite element simulations a linear two dimensional eigenvalue analysis is used. This method is especially suitable because it offers a very efficient modeling approach for this kind of application. The experimental data are based on measurements contained in previous publications by the authors. The comparison of the finite element simulations with the experimental data and the data from the analytical framework show that they are in good agreement. The results shown in this work serve to validate the numerical approach presented and allow for further, more complex simulations.

1 Introduction

Composite materials are of great relevance for lightweight constructions. One focus is on the combination of fiber-reinforced polymers (FRP) and metallic materials, so-called fiber metal laminates (FML). This material combination is particularly interesting for use in thin-walled components due to its high specific strength and stiffness, cf. [1, 2]. To manufacture FMLs, thin metal layers are integrated between layers of FRP. This results in structural components that are able to combine the advantages of the individual constituents. For example, components can be manufactured that benefit from the high ductility of the metal as well as the high specific strength of the FRP. This leads to advantages in many areas such as high damage tolerance [3, 4], load-bearing applications [5, 6], as well as for function integration [7] and structural robustness [8].

Because of the structure of these materials internal damage can occur without any externally visible indicators [3, 9, 10], similar to damage in components made of pure FRP. Therefore, in order to monitor these components, methods are needed that are capable of detecting this type of damage. A suitable method is based on guided ultrasonic waves (GUW), such as for example Lamb waves [11–13]. In order to perform such damage detection, knowledge of the propagation behavior of GUWs in FML is essential.

The integration of metal layers into FRP leads to abrupt stiffness variations across the thickness of FML and an even more anisotropic material behavior than it is already the case for pure FRP [14, 15]. The question arises, whether the known approaches for the propagation of GUWs in isotropic and transversely isotropic materials, cf. [16, 17], are applicable in this kind of material. In this regard, the literature shows that the approaches used for FRP can also be applied here. For example, Pant et al. [18] show that the dispersion relations obtained from the partial wave technique in combination with the Global Matrix Method (GMM) for FMLs consisting of aluminum and glass fiber-reinforced polymers (GFRP) can be confirmed with experimental results. Muc et al. [19] indicate for FML consisting of aluminum and carbon fiber-reinforced polymers (CFRP) and GFRP, respectively, that the results for the occurring group velocities of the stiffness matrix method in combination with finite element models (FEM) are in agreement with those obtained from experimental investigations. Mikhaylenko et al. [20] demonstrate that the results for the displacement fields for such waves agree between the results based on the numerical

* Corresponding author: e-mail barth@hsu-hh.de, phone +49 40 6541 2745, fax +49 40 6541 2034

Parameter	Value	Unit
E_1	122	GPa
$E_2 = E_3$	9.9	GPa
$G_{12} = G_{13}$	5.2	GPa
G_{23}	3.4	GPa
$\nu_{12} = \nu_{13}$	0.27	-
ν_{23}	0.47	-

Table 1: Material parameters for the CFRP layers, prepreg Hexcel Hexply 8552-AS4, see [27].

Parameter	Value	Unit
E	191	GPa
G	73.5	GPa
ν	0.3	-

Table 2: Material parameters for steel layers, steel 1.4310 (X10CrNi18-8).

solution of the analytical framework and those from FEM simulations. In addition, the work of Maghsoodi et al. [21] and Tai et al. [22] address the influence of damage in such material systems. The former is limited to numerical investigations, while Tai et al. are matching their results with experimental data. Studies on the behavior of interfaces between aluminum and FRP layers represent another area in which work on this topic can be found. For this purpose, Attar et al. [23] investigate the influence on the dispersion behavior of such a layer numerically and experimentally. Furthermore, LeCrom et al. [24] study the bonding layers between aluminum and applied CFRP patches under the consideration of shear-horizontal waves.

Based on these findings, this work will provide a deeper insight into the dispersion behavior of GUW in FML consisting of steel and CFRP. For this purpose, numerical and experimental results will be compared. The focus is on comparisons over large frequency ranges with high accuracy. To do this, existing experimental data from the authors [25] will be extended and compared with numerical finite element data from a two-dimensional eigenvalue analysis. The previous work shows that for wave propagation in fiber direction, the obtained experimental data are comparable to a numerical solution of the analytical framework using the GMM. These results are extended here to a comparison with a numerical solution using FEM and a propagation direction perpendicular to the fiber orientation.

An influence not initially considered in this work is the residual stresses in the material, resulting from heat treatments during manufacturing due to the different thermal expansion coeffients, see [26]. This influence will be considered in more detail in the further course of this research.

2 Material Definition

The material used in this work is a combination of CFRP prepreg (Hexcel Hexply 8552-AS4) layers and thin steel foils (1.4310). Four metal layers and twelve CFRP layers are stacked in a symmetrical pattern as follows $[\mathrm{St}/0_4/\mathrm{St}/0_2]_S$, see Fig. 1. The thicknesses of the steel layers is $0.12\,\mathrm{mm}$, while those of the CFRP layers is $0.13\,\mathrm{mm}$. This leads to a laminate thickness of $2.04\,\mathrm{mm}$ with a metal volume fraction of $24\,\%$.

Tab. 1 contains the used material parameters of the CFRP prepreg, taken from Johnston [27]. The suitability of these material parameters has been shown in previous work by the authors [25]. Additional sources for material parameters can also be found e. g. in [28–30]. The material parameters for the steel layers are taken from own test series and can be found in Tab. 2.

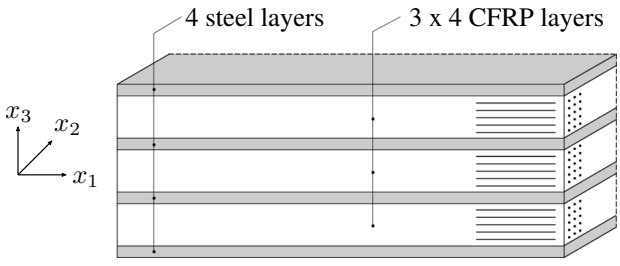

Fig. 1: Schematic structure of a FML specimen.

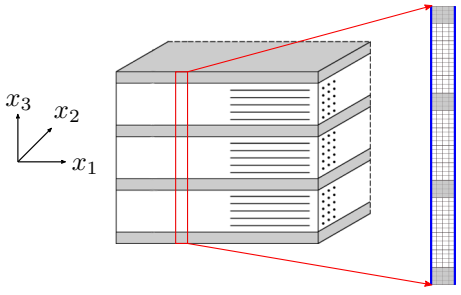

Fig. 2: Schematic representation of the FE model.

3 Finite Element Investigations

The following numerical approaches are based on the use of an eigenvalue analysis to calculate the dispersion relations of the GUWs under consideration. This method is known from the SAFE method [31–33] and offers a possibility to generate dispersion relations over large frequency ranges with little computational effort. Here, a fully linear numerical model is used for this analysis.

The method is based on a multiplicative split of the displacement field $\mathbf{u}$ of the waves into two parts, see [13]

$$\mathbf{u}\left(x_1, x_3, t, \omega, k\right) = \hat{\mathbf{u}}\left(x_3, \omega, k\right) e^{-i(kx_1 - \omega t)} \quad . \tag{1}$$

Here k represents the circular wave number in the propagation direction and ω the circular frequency of the propagating wave. The first part is a function only depending on the coordinate in thickness direction x_3 and thus describes a standing wave. The second part is a function depending on time and the propagation direction of the waves x_1 and describes the part of the propagating wave. It should be mentioned that Eqn. (1) is valid only if the displacement fields of the GUWs is decoupled from the coordinate x_2. Due to the orthotropy of the considered laminate this assumtion is valid for wave propagation in the fiber direction and perpendicular to it, see [11, Ch. 3].

Starting with the balance of linear momentum

$$\nabla \cdot \boldsymbol{\sigma} = \rho_0 \frac{\partial^2 \mathbf{u}}{\partial t^2} \quad , \tag{2}$$

where $\boldsymbol{\sigma}$ stands for the Cauchy stress tensor and ρ_0 for the density. The time derivative can be written using the displacement field from Eqn. (1) as

$$\rho_0 \frac{\partial^2 \mathbf{u}}{\partial t^2} = \rho_0 \, \omega^2 \, \mathbf{u} \quad . \tag{3}$$

Therefore, the implementation of Eqn. (2) into the framework of the finite element method leads to the eigenvalue problem

$$\left(\left[K\left(k\right)\right] - \omega^2 \left[M\right] \right) \left[d\right] = \left[0\right] \quad . \tag{4}$$

In it, $\left[K\left(k\right)\right]$ corresponds to the stiffness matrix as a function of the circular wavenumber k, $\left[M\right]$ to the mass matrix, and $\left[d\right]$ to the column matrix of displacements.

In the following, the solution of this eigenvalue problem is limited to the linear part. This is justified by the fact that the displacements of the wave motion are very small in comparison to the dimensions of the body and thus an influence of the deformation on the resulting circular wave number can be neglected.

3.1 Finite Element Model

Based on an eigenvalue analysis, only a one-dimensional model representing the cross-section in thickness direction x_3 of the laminate is required for the calculation of the dispersion relations in and perpendicular to the fiber orientation. However, during the course of this research, further effects will be considered, such as the presence of residual stresses from the manufacture of the laminate. To do this, the model has to be extended to two dimensions taking into account the propagation direction x_1 of the waves. In x_2-direction, a plane strain condition is assumed. Fig. 2 illustrates the discretized part of the structure, for which a $0.1\,\mathrm{mm}$ wide cross section of the laminate body is shown. In one-dimensional modeling, only the part of the displacement field that depends on the coordinate x_3 has to be analyzed, see equation (1). In the two-dimensional modeling, additional boundary conditions are required for the behavior in the direction of propagation. This is done by specifying periodic boundary conditions

$$\left[d\right]_{\text{right}} = \left[d\right]_{\text{left}} e^{-ik(x_{1\text{right}} - x_{1\text{left}})} \quad , \tag{5}$$

which represent the propagation of the wave in x_1-direction, see Eqn. (1). In this equation, the labels “left” and “right” represent the respective edges of the model in x_1 direction and are marked blue in Fig. 2.

For discretization, quadratic Lagrange elements are used. In thickness direction the metal and CFRP layers of the laminate are modeled separately, with no separate bonding layers between the individual layers. The CFRP layers are assumed to be homogeneous and transversely isotropic and are described using the material parameters given in Tab. 1.

4 Experimental Investigations

Within the scope of this work, only a brief description of the measurement procedure used to generate the experimental data can be provided. A more detailed insight into the setup and procedure of the measurements is given in previous work of the authors [25]. Therein also the reproducibility of these measurements with reference to measuring equipment and specimen shape is presented. The applied method uses a non-uniform two-dimensional discrete Fourier transform to evaluate the measurement data. The fundamentals regarding the use of a two-dimensional discrete Fourier transform to evaluate the measurement data of GUWs are based on [34, 35].

The experimental investigations are performed utilizing a rectangular plate specimen with dimensions $500\,\mathrm{x}\,500\,\mathrm{mm}$. For the excitation of the waves, rectangular piezoceramic actuators (ceramic type: PIC 255) with a L/W/T of $30\,\mathrm{x}\,5\,\mathrm{x}\,0.2\,\mathrm{mm}$ are adhesively applied to the surface of the specimen. To capture the wave motion, the resulting velocities of the material

points on the surface of the specimen are recorded by means of a Polytec PSV 500 laser scanning vibrometer. Due to a perpendicular alignment of the laser beam to the specimen surface, the out-of-plane velocities of the waves are measured to a predominant extent. The measurements record the motion of the waves along a measurement path in propagation direction, providing a measurement signal that is a function of time and the direction of propagation. To analyze the propagation in both directions considered in this work, the process is performed for a propagation direction parallel as well as perpendicular to the fiber orientation. Furthermore, in order to cover a large frequency range, multifrequency excitation signals are used. The measurements are performed in a frequency range between $0.002\,04\,\mathrm{MHzmm}$ and $2.04\,\mathrm{MHzmm}$. The resulting data are then transferred into the frequency-wavenumber domain by means of a two-dimensional discrete Fourier transformation, where frequency-wavenumber pairs can be identified on the basis of the occurring amplitude maxima. These identified pairs form the dispersion relations of the GUWs.

5 Comparison of Numerical and Experiamental Results

In the following, the dispersion relations from the FEM solutions are compared with those from the numerical solution of the analytic framework and those from the experiments. This is done by comparing the phase velocity-frequency relations. Based on the results in [20,25] on the dispersion behavior and the displacement fields of the two modes considered here, these modes are referred to as the fundamental symmetric mode S_0 and fundamental antisymmetric mode A_0. For the computation of the data from the analytical framework, it is refered to [25]. As for the FEM solutions, the underlying material parameters for the analytic framework correspond to those provided in Tab. 1.

Fig. 3 shows the resulting dispersion relations from FEM solutions and the analytic framework for the S_0 and A_0 modes. A propagation in and perpendicular to the fiber direction is considered. The comparison shows that both numerical methods provide identical results.

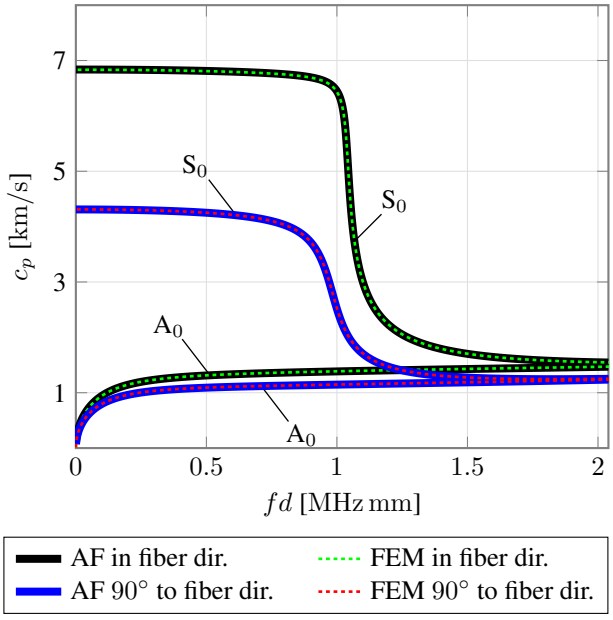

Fig. 3: Comparison between the dispersion behavior from FEM solutions and the numerical solution of the analytic framework (AF). Wave propagation in and perpendicular to fiber direction.

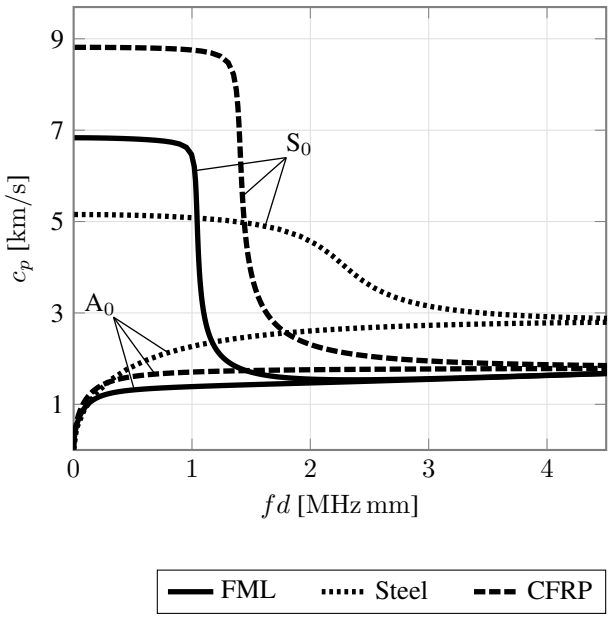

Fig. 4: Comparison between the dispersion behavior for FML, Steel and CFRP from FEM. Wave propagation in fiber direction.

On this basis, Fig. 5 holds a comparison between the experimental results and those from the FEM simulations for a wave propagation in fiber direction. The results show slight deviations, but the basic shapes of the propagation behavior are in good agreement. In Fig. 6 the same comparison for a propagation direction perpendicular to the fiber direction is depicted. Again, the basic shapes of the propagation behavior are in good agreement. However, the deviations between the graphs are more significant than in the fiber direction. Besides measurement uncertainties in the experimental data, there are additional influences from the experiments as well as from the numerical model that could contribute to the deviations that occur between the experimental and numerical data. On the experimental side, in addition to general manufacturing tolerances of the specimens, the influences of measurement inaccuracies in the alignment of the measurement path with respect to the real fiber direction and inaccuracies in the thickness distribution of the specimen should be mentioned in particular. In the context of the numerical model, the uncertainties from the material parameters used for the CFRP layers from the literature should be mentioned. In addition, the numerical model in its current form does not take into account residual stresses contained in the real specimen. A detailed evaluation of these influences cannot be carried out within the scope of this work. However,

the influence of the residual stress states on the wave propagation in particular will be the focus of subsequent work by the authors.

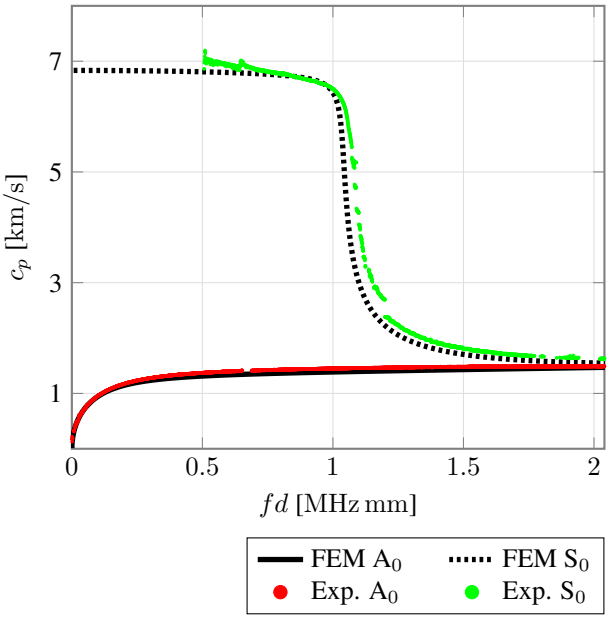

Fig. 5: Comparison between the dispersion curves from FEM and experiments. Wave propagation in fiber direction.

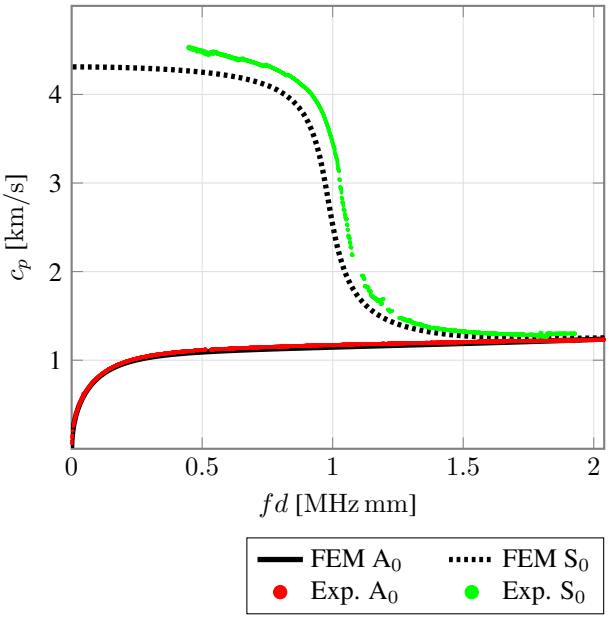

Fig. 6: Comparison between the dispersion curves from FEM and experiments. Wave propagation perpendicular to the fiber direction.

The experimental measurements used here, capture only the velocities of the material points on the surface of the specimen, i.e. on one of the steel layers. Therefore, it is not possible to verify on the basis of the measurement data alone whether the waves propagate only in this steel layer or throughout the entire thickness of the specimen. In Fig. 4 the dispersion relations from FEM solutions for FML, steel and CFRP are shown. Consequently, the good agreement between the numerical and experimental data in Fig. 5 and the large differences between a decoupled propagation in the outer steel layer in Fig. 4 indicate that the propagation of the waves take place over the entire thickness of the specimen. This conclusion is also supported by the numerically computed displacement fields of the fundamental wave modes in [20].

6 Conclusion

This work demonstrates that the nature of the dispersion relations, such as the multimodality, dispersivity, and the qualitative shape of the graphs for FML consisting of steel and CFRP ($[\mathrm{St}/0_4/\mathrm{St}/0_2]_S$) are in agreement between the experimental data, those from the FEM solutions and the numerical solution of the analytical framework. A comparison of the dispersion relationships between FML and a pure steel specimen also indicates that there is no decoupled propagation in the outer layer of the specimen. Therefore, it can be concluded that the propagation of the waves cover the entire thickness of the specimen. As a result it can be stated, that the occuring GUW show a similar propagation behavior as in pure FRPs.

Furthermore, causes for occurring deviations between the numerical and experimental results were identified. They can be found in the area of manufacturing as well as in the area of modeling. In the further course of this research, these influencing factors will be investigated in more detail. Therefore, e.g. the residual stresses will be added to the modeling approach, which serves to create a fundamental understanding of the influence of these stress states on the wave propagation.

Acknowledgements This work was conducted in the research group FOR 3022 'Ultrasonic Monitoring of Fibre Metal Laminates Using Integrated Sensors'. Financial support from the Deutsche Forschungsgemeinschaft (DFG) is gratefully acknowledged. Open access funding enabled and organized by Projekt DEAL.

References

[1] T. Sinmazçelik, E. Avcu, M. Ö. Bora, and O. Çoban, Mater Des **32**(7), 3671–3685 (2011).
[2] A. Vlot and J. W. Gunnink, Fibre Metal Laminates: An Introduction (Springer Netherlands, Dordrecht, 2001).
[3] G. B. Chai and P. Manikandan, Compos Struct **107**, 363–381 (2014).
[4] R. C. Alderliesten, M. Hagenbeek, J. J. Homan, P. A. Hooijmeijer, T. J. de Vries, and C. A. J. R. Vermeeren, Appl Compos Mater **10**(4/5), 223–242 (2003).
[5] A. Fink, P. P. Camanho, J. M. Andrés, E. Pfeiffer, and A. Obst, Compos Sci Technol **70**(2), 305–317 (2010).

[6] E. Petersen, D. Stefaniak, and C. Hühne, Compos Struct **182**(6), 79–90 (2017).
[7] A. Pototzky, D. Stefaniak, and C. Hühne, Potentials of load carrying conductor tracks in new vehicle structures, in: Technologies for economical and functional lightweight design, edited by K. Dröder and T. VietorZukunftstechnologien für den multifunktionalen Leichtbau (Springer Berlin Heidelberg, Berlin, Heidelberg, 2019), pp. 79–90.
[8] D. Düring, E. Petersen, D. Stefaniak, and C. Hühne, Compos Struct **238**, 111851 (2020).
[9] F. Morinière, R. Alderliesten, M. Tooski, and R. Benedictus, Cent Eur Jrnl Eng **2**(4), 1116 (2012).
[10] J. Bienias, P. Jakubczak, B. Surowska, and H. Debski, Proceedings of the ECCM16 - 16th Europ Conf on Compos Mater **16** (2014).
[11] R. Lammering, U. Gabbert, M. Sinapius, T. Schuster, and P. Wierach (eds.), Lamb-Wave Based Structural Health Monitoring in Polymer Composites, Research Topics in Aerospace (Springer International Publishing, Cham, 2017).
[12] F. G. Yuan (ed.), Structural health monitoring (SHM) in aerospace structures, Woodhead publishing series in composites science and engineering, Vol. number 68 (Woodhead Publishing is an imprint of Elsevier, Duxford, UK, 2016).
[13] V. Giurgiutiu, Structural health monitoring with piezoelectric wafer active sensors (Academic Press/Elsevier, Amsterdam, 2008).
[14] M. Abouhamzeh, Distortions and Residual Stresses of GLARE Induced by Manufacturing, Doctoral dissertation, Delft University of Technology, 2016.
[15] R. Alderliesten, Fatigue and fracture of fibre metal laminates, Solid mech and its appl, Vol. 236 (Springer, Cham, 2017).
[16] H. Lamb, Proceedings of the Royal Society of London. Series A, Containing Papers of a Mathematical and Physical Character **93**(648), 114–128 (1917).
[17] J. L. Rose, Ultrasonic Guided Waves in Solid Media (Cambridge Univ. Press, 2014).
[18] S. Pant, J. Laliberte, M. Martinez, and B. Rocha, Compos Struct **111**, 566–579 (2014).
[19] A. Muc, M. Barski, A. Stawiarski, M. Chwał, and M. Augustyn, Compos Struct **255** (2021).
[20] A. Mikhaylenko, N. Rauter, N. K. Bellam Muralidhar, T. Barth, D. A. Lorenz, and R. Lammering, Acoustics **4**(3), 517–537 (2022).
[21] A. Maghsoodi, A. Ohadi, M. Sadighi, and H. Amindavar, Jrnl Mech Sci Technol **30**(5), 2113–2120 (2016).
[22] S. Tai, F. Kotobuki, L. Wang, and A. Mal, Jrnl Nondestr Eval Diagn Progn Eng Syst **3**(4) (2020).
[23] L. Attar, D. Leduc, M. Kettani, M. Predoi, J. Galy, and P. Pareige, NDT and E Int **111**(04) (2020).
[24] B. Le Crom and M. Castaings, Jrnl Acoust Soc Am **127**(4), 2220–2230 (2010).
[25] T. Barth, J. Wiedemann, T. Roloff, T. Behrens, N. Rauter, C. Hühne, M. Sinapius, and R. Lammering, Preprint at https://arxiv.org/abs/2206.08934 (2022).
[26] J. Wiedemann, R. Prussak, E. Kappel, and C. Hühne, Compos Struct **Vol. 691**(1), 115967 (2022).
[27] A. A. Johnston, An integrated model of the development of process-induced deformation in autoclave processing of composite structures, PhD thesis, University of British Columbia, 1997.
[28] Hexcel Corporation, Product data sheet - HexPly 8552, 2016.
[29] T. Garstka, Separation of process induced distortions in curved composite laminates, PhD thesis, The University of Bristol, Bristol, 2005.
[30] E. Hörberg, T. Nyman, M. Åkermo, and S. Hallström, Compos Struct **209**(8), 499–507 (2019).
[31] Z. A. B. Ahmad, Numerical simulations of Lamb waves in plates using a semi-analytical finite element method, PhD thesis, Otto-von-Guericke-Universität Magdeburg, 2011.
[32] J. M. Galán and R. Abascal, Internat Jrnl for Num Meth in Engin **53**(5), 1145–1173 (2002).
[33] H. Gao, Ultrasonic guided wave mechanics for composite material structural health monitoring, PhD thesis, The Pennsylvania State University, 2007.
[34] D. Alleyne and P. Cawley, A two-dimensional Fourier transform method for the measurement of propagating multimode signals, J Acoust Soc Am, **Vol. 89**(3), 1159–1168 (1991).
[35] P. Hora and O. Červená, Determination of Lamb wave dispersion curves by means of Fourier transform, Appl. Comput. Mech., **Vol. 6**, 5–16 (2012).